applied sciences

MDPI

Article

Earthquake Prediction for the Düzce Province in the Marmara Region Using Artificial Intelligence

Turgut Pura [1,*], Peri Güneş [1], Ali Güneş [1] and Ali Alaa Hameed [2]

[1] Department of Computer Engineering, Istanbul Aydin University, Istanbul 34295, Turkey; parvanehshams@aydin.edu.tr (P.G.); aligunes@aydin.edu.tr (A.G.)
[2] Department of Computer Engineering, Istinye University, Istanbul 34396, Turkey; alaa.hameed@izu.edu.tr
* Correspondence: turgutpura@stu.aydin.edu.tr

Abstract: By definition, an earthquake is a naturally occurring event. This natural event may be a disaster that causes significant damage, loss of life, and other economic effects. The possibility of predicting a natural event such as an earthquake will minimize the negative effects mentioned above. In this study, data collection, processing, and data evaluation regarding earthquakes were carried out. Earthquake forecasting was performed using the RNN (recurrent neural network) method. This study was carried out using seismic data with a magnitude of 3.0 and above of the Düzce Province between 1990 and 2022. In order to increase the learning potential of the method, the b and d values of earthquakes were calculated. The detection of earthquakes within a specific time interval in the Marmara region of Turkey, the classification of earthquake-related seismic data using artificial neural networks, and the generation of predictions for the future highlight the importance of this study. Our results demonstrated that the prediction performance could be significantly improved by incorporating the b and d coefficients of earthquakes, as well as the data regarding the distance between the Moon and the Earth, along with the use of recurrent neural networks (RNNs).

Keywords: earthquake; recurrent neural network; prediction; artificial neural network

Citation: Pura, T.; Güneş, P.; Güneş, A.; Hameed, A.A. Earthquake Prediction for the Düzce Province in the Marmara Region Using Artificial Intelligence. *Appl. Sci.* **2023**, *13*, 8642. https://doi.org/10.3390/app13158642

Academic Editors: Artem Shikhovtsev and Pavel G. Kovadlo

Received: 5 June 2023
Revised: 19 July 2023
Accepted: 21 July 2023
Published: 27 July 2023

1. Introduction

Natural phenomena are in constant evolution. The earthquake monitoring agencies monitor these changes and the data obtained are recorded. One of the natural events is an earthquake [1]. Over the centuries, many large and small earthquakes have occurred in every corner of the world. These data are recorded in earthquake monitoring centers investigating seismic station's signals [2]. The recorded data are analyzed and scaled by seismologists [3]. However, when an earthquake occurs, the magnitude can be calculated precisely. Aftershocks can affect the calculation of magnitude, as they could cover part of the signal that maybe used to calculate the magnitude [4].

There is still the need for a straightforward method for earthquake prediction and pre-scaling. This is because it is tough to predict an earthquake due to the uncertainty of the event and its sudden occurrence [5]. Many methods, probability calculations, algorithms, and analysis techniques have been used to predict earthquakes. Artificial intelligence methods and machine learning are most commonly used in earthquake prediction [6]. However, in engineering, as in many other fields, artificial intelligence is used effectively on big data [7]. The examination of research in recent years shows that artificial intelligence is used to predict human or natural events and solve problems in different fields [8]. The distribution of the data to be used during the estimation according to time and classification are essential. Time distribution is a technique primarily used in data classification. We can call it a "time series", a data collection organized in a chronological order [9]. It provides an opportunity to evaluate and analyze the data generated using a series [10].

In this study, seismic data from the Düzce Province in Turkey, covering the years 1990–2022, were utilized. Düzce Province was selected due to it being located on the North

Anatolian Fault Zone, which is a primary seismic region, and because of the limited number of studies conducted in this area. The accuracy rates were improved by calculating the b and d coefficients of the seismic data. The data were subjected to prediction and testing processes using the RNN method. The results were compared with the actual data.

2. Related Studies

Many methods, analyses, and results have been used for prediction. Some of these results approached the goal and while others did not. After the literature analysis, the studies that most closely approached the goal were selected and are listed in Table 1.

Table 1. Literature review table.

Article	Authors	Date
Earthquake Forecasting Using Neural Networks: Results and Future Work.	Alves, E. I. [11]	2006
Neural Network Models for Earthquake Magnitude Prediction Using Multiple Seismicity Indicators.	Panakkat, A. and Adeli, H. [12]	2007
A Probabilistic Neural Network for Earthquake Magnitude Prediction.	Adeli, H. and Panakkat, A. [13]	2009
Artificial Neural Networks for Earthquake Prediction Using Time Series Magnitude Data or Seismic Electric Signals.	Moustra, M., Avraamides, M. and Christodoulou, C. [14]	2011
Yapay Sinir Ağı Yöntemiyle Deprem Tahmini: Türkiye Batı Anadolu Fay Hattı Uygulaması.	Çam, H. and Duman, O. [15]	2016
Kastamonu ve Yakın Çevresi İçin Deprem Olasılığı Tahminleri	Özmen, B. [16]	2011
Natural Time Analysis of Global Seismicity.	Christopoulos, S. R. G., Varotsos, P. K., Perez-Oregon, J., Papadopoulou, K. A., Skordas, E. S. and Sarlis, N. V. [17]	2022
Forecasting Earthquakes: The RELM Test.	Sachs, M., Turcotte, D. L., Holliday, J. R. and Rundle, J. [18]	2012
Estimation of the Size of Earthquake Preparation Zones.	Dobrovolsky, I. P., Zubkov, S. I. and Miachkin, V. I. [19]	1979
SafeNet: SwArm for Earthquake Perturbations Identification Using Deep Learning Networks.	Xiong, P., Marchetti, D., De Santis, A., Zhang, X. and Shen, X. [20]	2021
Possible Earthquake Forecasting In a Narrow Space-Time-Magnitude Window.	Florios, K., Contopoulos, I., Tatsis, G., Christofilakis, V., Chronopoulos, S., Repapis, C. and Tritakis, V. [21]	2021

In a 2006 study, Alves was one of the first to propose the use of artificial neural networks for earthquake prediction [11]. The author, E.I. Alves, was inspired by the successful application of similar approaches to financial forecasting tasks, which are similar to seismic activity in their chaotic nature. He tested this method on seismic data from the Azores region, Portugal. E. I. Alves scientifically stated that he predicted the earthquakes in July 1998 (MMI = 8) and January 2004 (MMI = 5) correctly. However, it was not assessed using any statistical measurement. Therefore, the performance of this approach is yet to be evaluated objectively.

In the studies by Panakkat and H. Adeli in 2007 and in 2009, the problem of earthquake prediction was organized in terms of output classes with the largest seismic magnitude ranges in a predefined time series [12]. They used this dataset to estimate the magnitude of the largest earthquake in a predefined region for the next month. They prepared eight

mathematically calculated "seismicity indicators" that can be used to evaluate the seismic potential of a region [13]. The authors proposed the architecture of a probabilistic neural network (PNN) for prediction using the formulas they created. The model has been tested on data for the Southern California seismic region (33.8–35.4° N and 114.75–119.25° W) and has been proven to provide good prediction accuracy for earthquakes of magnitude 4.5–6.0. However, the PNN did not perform satisfactorily for earthquakes greater than magnitude 6.0.

M. Moustra et al. evaluated the accuracy of the neural network for earthquake prediction using different inputs [14].

1. The first case study focuses on estimating the next day's biggest seismic event using only time series earthquake magnitude data;
2. The latter study focuses on the use of seismic electrical signals (SES) to predict the magnitude of the next seismic event.

For the first case, a feedforward backpropagation neural network is used. An input file contains the maximum size value for each day. The accuracy rate resulting from the model was stated as 58.02%. In the second case, ANN was used to generate the lost data using magnitude time series. The accuracy of the size estimation was stated to be just over 60% in the initial dataset.

Handan Çam and Osman Duman, in their 2016 study, "Earthquake Prediction with Artificial Neural Network Method: Turkey West Anatolian Fault Line Application", used a generalized method to predict in advance, with certainty, the location and time of earthquakes that have not yet been discovered [15]. In this study, a feedforward backpropagation artificial neural network based on the b value of the Gutenberg–Richter relationship was developed for performing the predictions. The artificial neural network was trained using earthquake data from four regions with intense seismic activity in western Turkey. After the training phase, earthquake data from later dates for the same regions were used for testing, and the network's success was demonstrated.

In his 2011 study, titled "Earthquake Probability Estimates for Kostamonu and Its Surroundings", Özmen, B. examined the city of Kastamonu, which is located in the first-degree earthquake zone [16]. The seismicity of Kastamonu was investigated using earthquake data with a magnitude of $M \geq 4.0$ that occurred between 1900 and 2011, which fell within the region drawn 150 km from the city center. Most earthquakes occurred on the North Anatolian Fault Zone, the Dodurga fault, the Eldivan-Elmadağ tectonic wedge, the Merzifon fault, and the Taşova-Çorum fault zone in the south of Kastamonu. This study used earthquake data with $M \geq 4.0$, which occurred in circular areas drawn to surround the Kastamonu city center for 50, 100, and 150 km and accepted as seismotectonic zones. It aims to find the a and b parameters in the Gutenberg–Richter magnitude–frequency relation for each region. Using these parameters and the Poisson model, it is possible to predict the probability of earthquakes of different magnitudes and their return periods. The earthquake probabilities of each region are calculated for earthquakes in 10, 20, 30, 40, 50, 75, and 100 years and with magnitudes of 5.0, 5.5, 6.0, 6.5, 7.0, and 7.5.

Christopoulos et al. [17] investigated the "Natural time" of seismicity and identified an order parameter for the seismic events. Upon examining the earthquakes in the recent years, significant progress has been observed in the natural time analysis of seismicity. These advancements encompass the identification of distinct minima of the $\kappa 1$ order parameter in seismicity on both regional and global scales, the emergence of a correlation between the time correlations of earthquake magnitude time series and these minima, and the introduction of EQ nowcasting by Turcotte, Rundle, and their colleagues [18]. The researchers have implemented these recent advancements in the analysis of global seismicity using the Global Centroid Moment Tensor (GCMT) catalog. The findings demonstrate that the combined effect of these three milestones can furnish valuable preliminary information regarding the timing and epicenter location of powerful earthquakes with magnitudes of $M \geq 8.5$ in the GCMT. The results exhibit notable statistical significance (with p values

on the order of 10^{-5} while the epicentral regions comprise only 4% of the investigated area) [18].

In their study, Xiong et al. investigated numerous ionospheric disturbances that occur as a result of significant earthquake activity observed with the SwArm satellite. This study utilized the SafeNet deep learning framework. The system was trained using earthquake data from the period of 2014 to 2020, specifically focusing on earthquakes with magnitudes of 4.8 or greater. The findings revealed that nighttime data, collected within a circular region centered at the epicenter utilizing a radius and input window size of 70 consecutive data points as defined by Dobrovolsky [19], exhibited the highest performance in effectively identifying pre-earthquake perturbations [20].

In 2021, Florios et al. studied earthquake prediction in a limited period, wherein an extended time series of Schumann Resonance records were analyzed using two multiparametric statistical methods. The methods used to test their potential are linear logistic regression (LogReg) and nonlinear random forest (R.F.) [21]. The analysis examined events with a 48 h magnitude window, at least 250 km from the observatory, and with a magnitude greater than four on the Richter scale. The LogReg method defines the magnitude of the signal within 10 min of the recording intervals as the main seismic reporting parameter. The R.F method has been shown to produce promising results, which will be improved by continuously enriching the operational data with new data.

Many classifications, data sets, locations, and approaches have been used in earthquake predictions. In this study, the Düzce Province, geographically located in the Marmara region of Turkey, with GPS coordinates of $40°49'59''$ N and $31°10'0''$ E was selected. The Düzce Province was selected as the study area because it is a province with intense earthquake activity.

The purpose of this study is to determine earthquakes' magnitudes and their occurrence probability in the future using earthquake magnitude data, including the Moon's distance from the Earth, the b value and d value of the earthquakes, the depth and time information of the region between the years 1990 and 2022, by applying the RNN method.

3. Materials and Method

This section contains information about the research model, research variables, data collection instruments, experimental process, data preparation and analysis, estimation instrument, and data interpretation.

3.1. Calculation of Earthquake's Magnitude

To calculate an earthquake's magnitude, primary (P) and secondary (S) waves are evaluated using formulas and the magnitude of the earthquake is scientifically derived [22]. In P or compressional waves, the vibration of the rock occurs in the direction of propagation. The P waves are the fastest propagating waves in the ground and consequently the first to be detected via seismometers [23].

The velocity of P waves in such a medium is obtained using Equation (1) [23].

$$Vp = \sqrt{\frac{(\lambda + 2\mu)}{\rho}} \tag{1}$$

where μ is the shear modulus (modulus of rigidity, sometimes denoted as G and also called the second Lamé parameter), ρ is the density of the material through which the wave propagates, and λ is the first Lamé parameter.

In S or shear waves, the rock vibrates perpendicularly to the direction of wave propagation. In ground, the S waves usually propagate about 60% as fast as P waves, and the S wave always follows the P wave in Equation (2) [24].

$$Vs = \sqrt{\frac{\mu}{\rho}} \tag{2}$$

In the first phase, the time from the beginning of the P waves to the beginning of the S waves is calculated, the nomogram is marked, and the corresponding km value is read. It is the distance of the station from the epicenter.

In the second step, the amplitude of the strongest S wave is measured and plotted on the nomogram. The first two signs are combined linearly. An earthquake's magnitude is where the line connecting these two signs crosses the scale.

This method calculated the earthquakes of magnitudes 3 and above ($M \geq 3$) that occurred in the Düzce Province between 1990 and 2022. The 1-year dataset for 1990 is shown in (Table 2).

Table 2. Earthquakes in the Düzce Province in 1990 ($M \geq 3$).

Date	Month	Day	Local Time	Latitude	Longitude	Depth	Magnitude
1990	February	09	18:20:00.00	41.0000	31.9000	10	3.7
1990	February	14	12:17:01.40	40.7400	29.1000	7	3.0
1990	April	11	08:02:08.00	40.7000	29.9000	7	3.0
1990	May	06	22:09:13.60	40.7200	29.7000	13	3.1
1990	May	07	10:36:02.70	40.5800	30.2000	5	3.5
1990	June	07	23:28:30.00	40.7400	29.2000	10	3.3
1990	June	08	01:47:56.00	40.5400	30.1400	3	3.9
1990	June	18	19:27:08.00	40.5100	30.5000	5	3.3
1990	July	21	17:56:49.00	40.7000	30.3000	22	3.1
1990	August	22	13:02:34.00	41.0000	29.9000	3	3.1
1990	September	01	17:27:37.00	40.7000	30.0000	8	3.0
1990	September	29	00:02:17.00	40.7000	29.8000	12	3.0
1990	October	03	01:51:29.00	40.6900	30.0000	5	3.0
1990	October	05	10:16:45.00	40.7000	30.0000	7	3.0
1990	October	08	05:50:14.00	40.7000	30.2000	4	3.1
1990	October	19	05:28:11.00	40.6800	30.0000	7	3.0
1990	November	04	08:07:49.70	40.7800	30.0300	9	3.1
1990	November	11	22:06:00.10	40.6000	31.7400	14	3.2

The 33-year histogram distribution highlighting the number corresponding to the size of the earthquake dataset is shown in Figure 1.

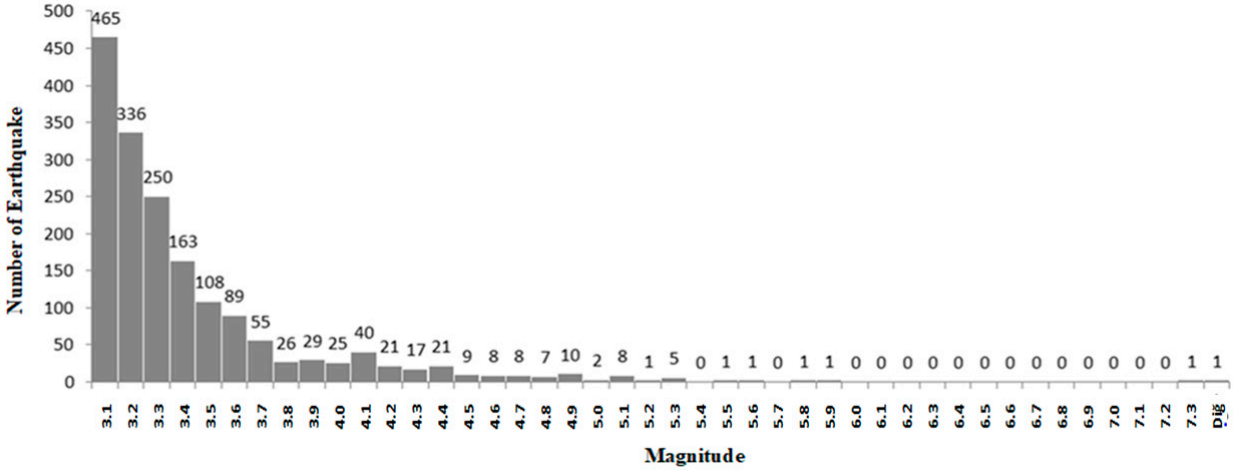

Figure 1. Earthquakes' magnitude distribution.

The earthquakes' time, location, and depth were added to the record. The Kandilli Observatory Earthquake Research Institute provided us with the seismic data.

3.2. Distance of the Moon from Earth

The distance of the Moon from the Earth is obtained using a formula that calculates the varying distance along the axes of the Moon's orbit around the Earth [25]. The formula is as follows (3).

$$\text{Distance} = \sqrt{[(x2 - x1)^2 + (y2 - y1)^2 + (z2 - z1)^2]} \quad (3)$$

In this formula, (x1, y1, and z1) represent the coordinates of the center of the Earth, and (x2, y2, and z2) represent the coordinates of the center of the Moon, respectively. The coordinates are typically presented in a three-dimensional Cartesian coordinate system. It is important to note that the distance between the Earth and the Moon is not constant due to their elliptical orbits and various factors such as gravitational interactions with other celestial bodies. The average distance is approximately 384,400 km or 238,900 miles. The formula used to obtain this distance takes into account the fact that the Moon's orbit around the Earth is elliptical and is related to the varying distance of the Moon along the axes of its orbit around the Earth [26].

The average distance of the Moon from the Earth, based on the dates and locations of earthquakes in the Düzce Province between 1990 and 2022, can be found on the website timeanddate.com [27].

3.3. B Value and D Value Calculation

The b value of an earthquake indicates the average intensity of earthquakes occurring in an earthquake area during a measurement period. The d value, on the other hand, indicates the total intensity of earthquakes occurring in an earthquake area [28].

The difference between the b and d values is that while the former represents the number of earthquakes occurring in an earthquake zone, the latter represents the total intensity of those earthquakes. If the number of earthquakes in an earthquake zone is high, the b value may be high and the d value may be low. In this case, earthquakes of low intensity are frequent in that earthquake zone. If the total intensity of earthquakes occurring in an earthquake zone is high, the d value may be high, while the b value may be low [29]. In this case, rare but high-intensity earthquakes may occur in that earthquake zone.

The b value of an earthquake is a parameter used to measure the ratio between the number of higher and lower magnitude events. The b value is calculated using the formula in Equation (4) [30].

$$b = \log10\ (N + C) \quad (4)$$

where N is the number of earthquakes occurring in an earthquake zone and C is a constant value. A high b value means that frequent earthquakes of high intensity occur in the earthquake zone. A low b value means that earthquakes of low intensity occur in the earthquake zone.

To calculate the b value, the number of earthquakes (N) occurring in the earthquake zone was determined first. Then, the constant value (C) was added, and the b value was calculated using the aforementioned formula. All the calculated b values were included in this study as a dataset.

To calculate the d value, the formula in Equation (5) [31] was used.

$$d = \log10\ (D + C) \quad (5)$$

where D is the total intensity of earthquakes occurring in an earthquake zone and C is a constant value. A high d value means that earthquakes occurring in the earthquake zone are generally of high intensity. A low d value means that earthquakes occurring in the earthquake zone are generally of low intensity.

To calculate the "d" value using the formula, d = log10 (D + C), one needs to obtain specific values for D (distance) and C (constant). The formula that we have used here

highlights a logarithmic relationship between the distance value (D) and the constant value (C).

In earthquake seismology, the Richter scale or other such scales are commonly used to measure earthquakes' magnitude. These scales take into account factors such as the amplitude of seismic waves recorded with seismographs.

To calculate the d values, the total intensity (D) of the earthquakes occurring in a zone is first calculated. Then, the constant value (C) is added and the d value is calculated using the aforementioned formula. The calculated d values were added to this study as a dataset.

3.4. RNN (Recurrent Neural Network)

RNN is an artificial intelligence (A.I.) method. It is an artificial neural network that considers input data's order and timing and is very good at estimating the relationship between data. Due to this property, RNN is widely used in machine learning applications [32].

The RNN working algorithm includes the following steps.

(a) The input data are entered into the input layer;
(b) The input data are processed in the hidden layers and the weights are learned;
(c) The hidden layers process the data and generate the output data;
(d) The output data are sent to the output layer;
(e) The output data are generated.

RNNs use the formulas shown in (Table 3) when processing data [33].

Table 3. RNN formulas.

Formulas	Explanation
$h_t = f(h_{t-1}, X_t)$	h_t: current value of h h_{t-1}: the previous h value x_t: current input vector
$h_t = \tanh(W_{hh}h_{t-1} + W_{hx}X_t)$	W: weight h: hidden layer W_{hh}: weight of the previous hidden layer W_{hx}: weight of the current hidden layer tanh: activation function
$y_t = W_{hy}h_t$	W_{hy}: weighing value of the output layer y_t: output

The primary purpose of this study is to predict future earthquakes with the RNN model, using past earthquakes and other data as inputs to build an earthquake prediction model. The data used in the study include the magnitude, location, time, depth, b and d values of the earthquakes, and the distance of the Moon from the Earth. By processing these sequential data, the RNN model will predict the time, location, and probability of possible earthquakes in the future.

A 33-year dataset was used to train the RNN model and test its predictions.

RNN and Other Methods

There are many machine learning methods that work on a similar logic to RNN. In addition to RNN, the most commonly preferred methods are XGBoost, Prophet, and ARIMA.

XGBoost (Extreme Gradient Boosting) is a powerful boosting algorithm widely used in the field of machine learning. Boosting is an ensemble learning technique that aims to combine weak learners (e.g., decision trees) to create a strong learner. XGBoost is specifically designed to achieve successful results in classification and regression problems using this ensemble method [34].

Prophet is an open-source time series analysis library developed by Facebook. It can be used in both R and Python programming languages. Prophet is designed to perform predictions in complex time series data with features such as seasonality, holiday effects,

and other time-related patterns. It is popular due to its ease of use and effective results, commonly used in various domains such as business analytics, demand forecasting, financial analysis, and social media data analysis [35].

ARIMA (AutoRegressive Integrated Moving Average) is a statistical model used to analyze and perform predictions in time series data. The ARIMA model captures structural features in time series data (auto-regression, moving average, and integration) [36].

In general, ARIMA is a fundamental statistical model effective for stationary time series data, while Prophet is suitable for time series data with complex features, such as seasonality. XGBoost is preferred for classification and regression tasks with non-structural data, and RNN is used for handling time-dependent data and capturing relationships over time. The choice of method depends on the data structure, analysis goals, and characteristics of the dataset. In this study, the RNN method was applied to the dataset used.

4. Experimental Datasets

Based on previous studies, we carried out adjustments and additions to our dataset. The seismic data (earthquake magnitude, latitude, longitude, and depth) were provided by the Kandilli Observatory. The seismic data contain records of earthquakes with magnitudes of 3 and above that occurred between 1990 and 2022 in the Düzce Province in the Marmara region.

In the estimation phase, the seismic data are used to train and test the model. RNN was used as the model. To increase the robustness of the model, the distance of the Moon from the Earth, which is assumed to be effective in the formation of an earthquake, is added. The b value and d value are calculated for each earthquake that occurred within the 33 years which had a magnitude greater than 3.0 and are used as another dataset and included in the model.

To test the accuracy of the model, first, the earthquakes that occurred in November and December 2022 were compared to the data predicted using the model. Second, the August 1999 earthquakes with higher intensity were compared with the data estimated using the model.

5. Results and Discussion

This section contains the results of the estimation of earthquake probability and magnitude between 1990 and 2022 for the Düzce Province. The first study was conducted for the earthquakes occurring in November and December 2022. Seven hundred fifty-six earthquakes with magnitudes between 1.0 and 6.1 occurred in this indicated period. Of the earthquakes that occurred, 16 were with magnitudes of 3.0 and above and are shown in Figure 2.

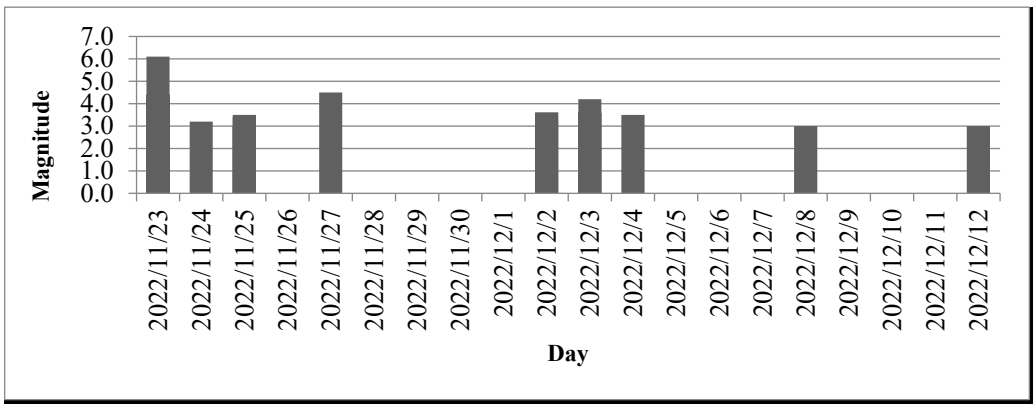

Figure 2. Earthquake distribution in Düzce in November and December.

The earthquake's magnitude, depth, location, time, the distance of the Moon from the Earth, b value, and d value were used in the training and testing phase of the RNN model.

The estimation phase was studied using earthquakes with magnitude three and above that occurred in the Düzce Province in November and December. The estimated magnitudes and probability values were compared with the actual data.

The estimated earthquakes' magnitudes are shown in Figure 3.

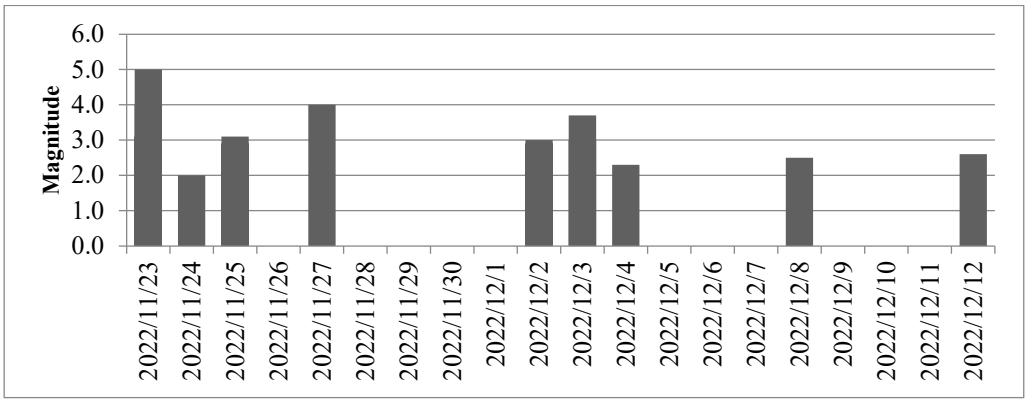

Figure 3. Estimated distribution of earthquakes' magnitudes.

An examination of the results shows a highest probability of 75.3% and a lowest probability of 58.9% for an earthquake between the actual data and the estimated data. These probabilities likely refer to the likelihood or confidence level associated with the similarity between the actual earthquake data and the estimated data. Compared to the estimated earthquakes' magnitudes, the actual earthquakes' magnitudes were estimated with a maximum error rate of 0.5% and a minimum error rate of 0.4%. The actual sizes and the probable and prospective sizes are shown in Table 4 and Figure 4.

Table 4. Predicted and current earthquake data.

Date	Magnitude (M $\geq$ 3)	Depth (km)	Probability (%)	Prediction (M)
23 November 2022	6.1	8.3	73.0	5.6
23 November 2022	4.4	5	75.3	4.0
23 November 2022	3.8	5.3	73.2	3.1
24 November 2022	3.2	3.8	60.7	2.7
25 November 2022	3.5	5	65.4	3.1
25 November 2022	3.4	5	60.2	2.9
25 November 2022	3	6.5	63.4	2.6
27 November 2022	4.5	17.5	73.2	4.0
2 December 2022	3.6	9.9	74.1	3.1
2 December 2022	3.6	5.1	72.2	3.1
2 December 2022	3.3	8.3	73.4	2.8
3 December 2022	4.2	10.6	69.2	3.7
3 December 2022	3.6	14.1	71.3	3.1
4 December 2022	3.5	6.3	58.9	3.0
8 December 2022	3	5.4	63.4	2.5
12 December 2022	3	4.5	66.9	2.6

The second study was conducted for August 1999, when 19 earthquakes occurred in Düzce and caused great destruction. In order to evaluate the period before and after the earthquakes, the months of July, August, and September were studied. An earthquake magnitude estimation study was conducted in August. A total of 295 earthquakes with magnitudes of 3.0 and above occurred within the specified 3-month period. Of the earthquakes experienced, 141 earthquakes occurred in August. The diurnal distribution of the earthquakes in August is shown in Figure 5.

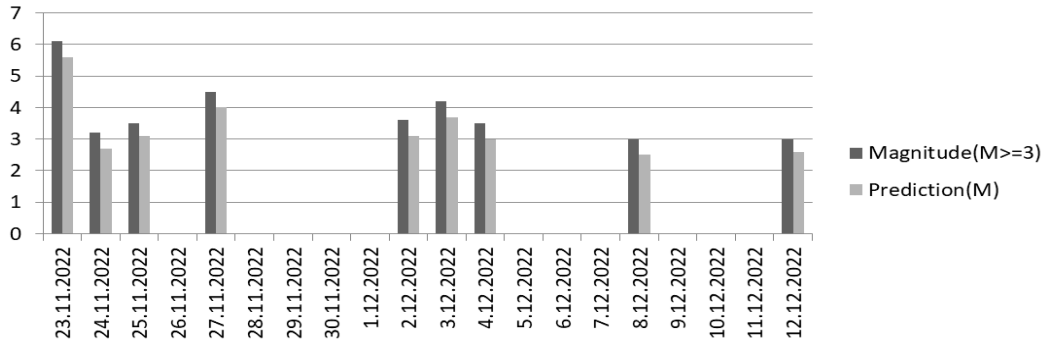

Figure 4. Predicted magnitude vs. real magnitude.

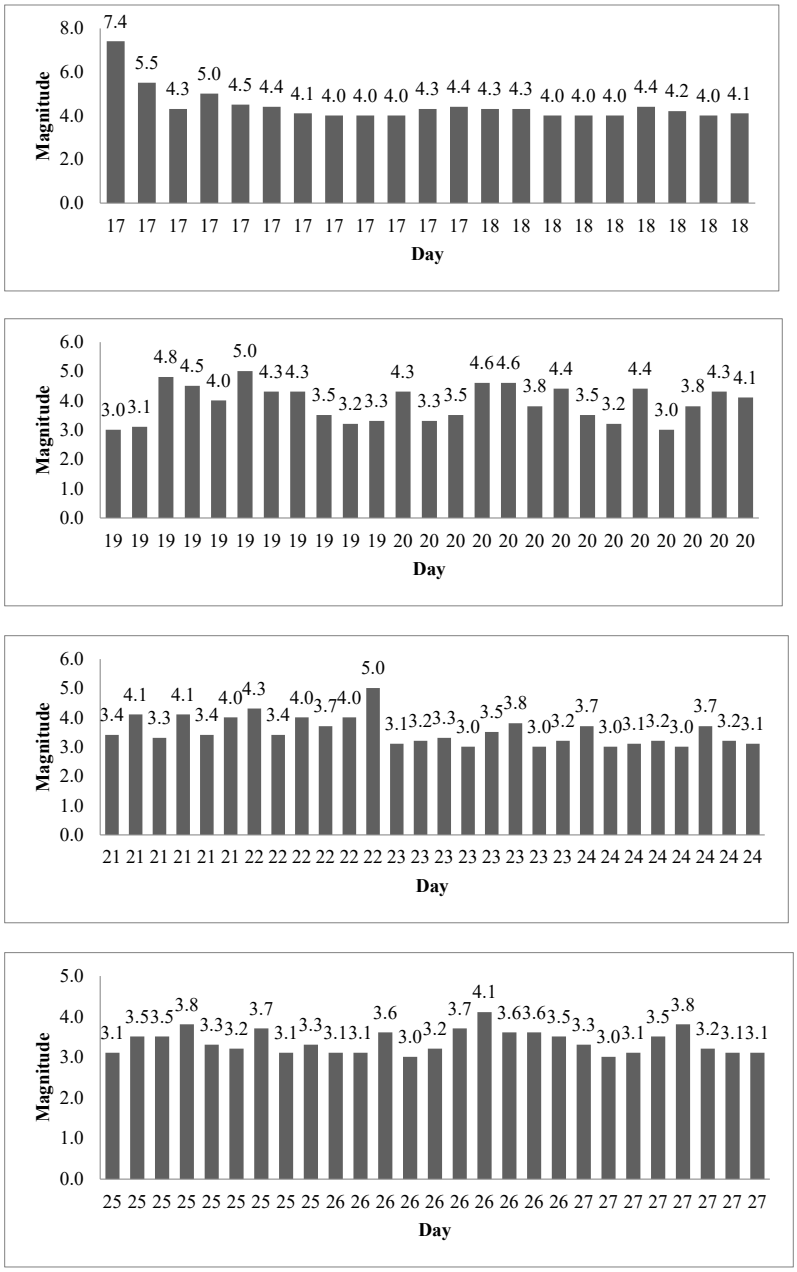

Figure 5. *Cont*.

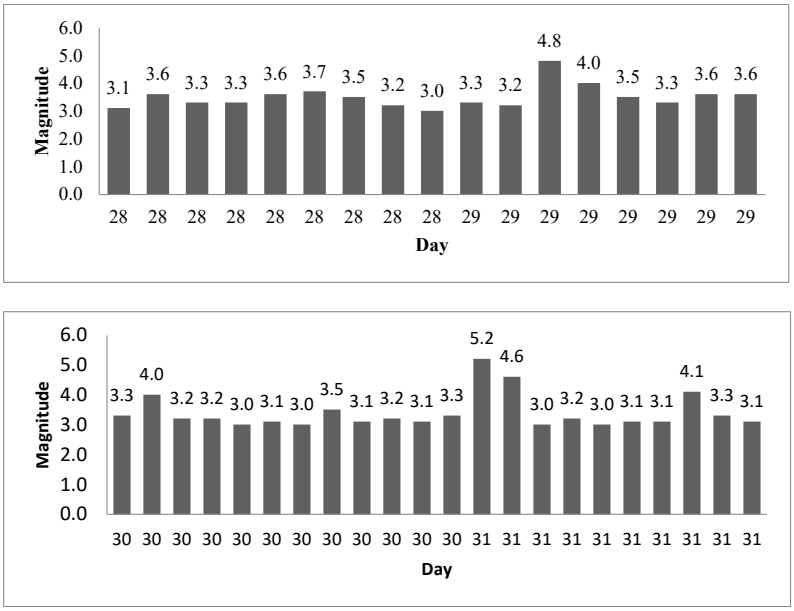

Figure 5. Earthquake distribution in Düzce in August 1999.

The estimation phase study was carried out using the RNN method for earthquakes with magnitude three and above in August 1999 in Düzce. The estimated magnitude and probability values were compared with the actual data.

The estimated earthquakes' magnitudes are shown in Figure 6 and estimated earthquakes' magnitudes vs. real magnitudes are shown in Figure 7.

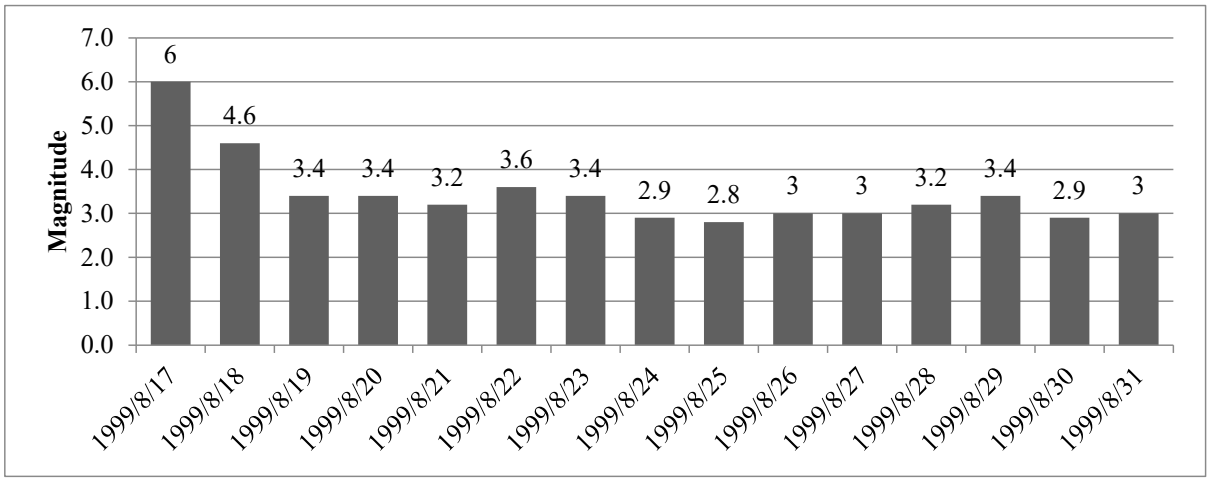

Figure 6. Estimated magnitude data.

An examination of the obtained results shows that between the real data and the estimated data the highest probability of an earthquake is 74.3% and the lowest is 68.3%. In the month of August, a minimum of 6 and a maximum of 14 earthquakes occurred per day. The average earthquakes' magnitudes per day is presented in (Table 5).

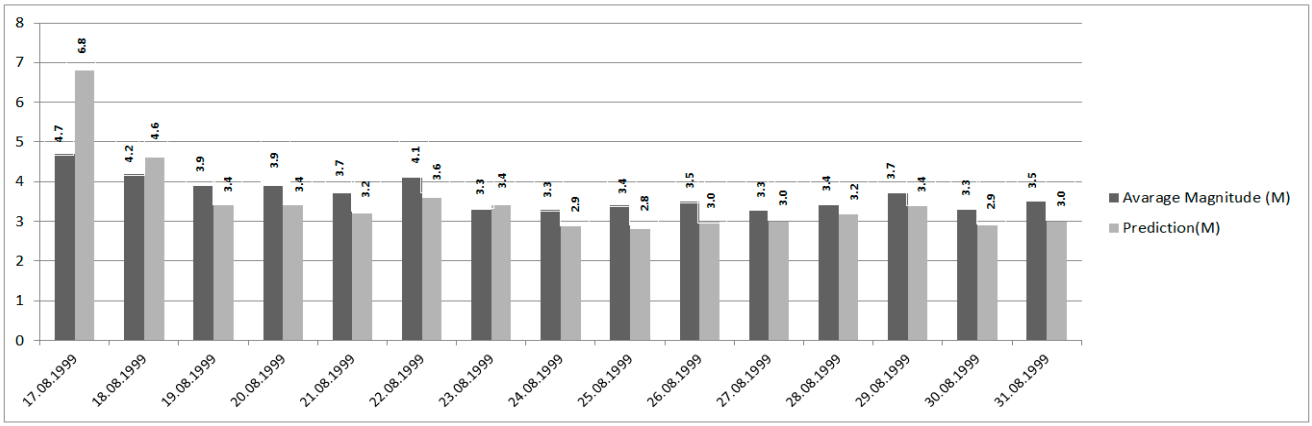

Figure 7. Comparison between the predicted magnitude and the real magnitude from 17 August to 31 August 1999.

Table 5. Actual and estimated magnitude data for 17 August 1999.

Date	Depth (km)	Magnitude ($M \geq 3$)	Average Magnitude ($M \geq 3$)	Probability (%)	Prediction (M)
17 August 1999	18	7.4	4.7	74.3	6.8
17 August 1999	15	5.5			
17 August 1999	5	4.3			
17 August 1999	16	5.0			
17 August 1999	16	4.5			
17 August 1999	17	4.4			
17 August 1999	10	4.1			
17 August 1999	11	4.0			
17 August 1999	6	4.0			
17 August 1999	13	4.0			
17 August 1999	16	4.3			
17 August 1999	16	4.4			

Compared to the estimated earthquakes' magnitudes that occurred on a given day, the actual earthquakes' magnitudes were estimated with a maximum error rate of 0.6% and a minimum error rate of 0.1%.

The actual magnitude data, probability, and predicted magnitudes are shown in Tables 5–19.

Table 6. Actual and estimated magnitude data for 18 August 1999.

Date	Depth (km)	Magnitude ($M \geq 3$)	Average Magnitude ($M \geq 3$)	Probability (%)	Prediction (M)
18 August 1999	14	4.3	4.2	74.0	4.6
18 August 1999	5	4.3			
18 August 1999	5	4.0			
18 August 1999	9	4.0			
18 August 1999	8	4.0			
18 August 1999	11	4.4			
18 August 1999	9	4.2			
18 August 1999	1	4.0			
18 August 1999	24	4.1			

Table 7. Actual and estimated magnitude data for 19 August 1999.

Date	Depth (km)	Magnitude (M $\geq$ 3)	Average Magnitude (M $\geq$ 3)	Probability (%)	Prediction (M)
19 August 1999	10	3.0	3.9	72.2	3.4
19 August 1999	3	3.1			
19 August 1999	6	4.8			
19 August 1999	12	4.5			
19 August 1999	14	4.0			
19 August 1999	11	5.0			
19 August 1999	12	4.3			
19 August 1999	1	4.3			
19 August 1999	9	3.5			
19 August 1999	28	3.2			

Table 8. Actual and estimated magnitude data for 20 August 1999.

Date	Depth (km)	Magnitude (M $\geq$ 3)	Average Magnitude (M $\geq$ 3)	Probability (%)	Prediction (M)
20 August 1999	11	4.3	3.9	70.4	3.4
20 August 1999	5	3.3			
20 August 1999	14	3.5			
20 August 1999	8	4.6			
20 August 1999	17	4.6			
20 August 1999	12	3.8			
20 August 1999	7	4.4			
20 August 1999	5	3.5			
20 August 1999	9	3.2			
20 August 1999	16	4.4			
20 August 1999	21	3.0			
20 August 1999	8	3.8			
20 August 1999	9	4.3			
20 August 1999	1	4.1			

Table 9. Actual and estimated magnitude data for 21 August 1999.

Date	Depth (km)	Magnitude (M $\geq$ 3)	Average Magnitude (M $\geq$ 3)	Probability (%)	Prediction (M)
21 August 1999	8	3.4	3.7	71.5	3.2
21 August 1999	8	4.1			
21 August 1999	7	3.3			
21 August 1999	1	4.1			
21 August 1999	1	3.4			
21 August 1999	23	4.0			

Table 10. Actual and estimated magnitude data for 22 August 1999.

Date	Depth (km)	Magnitude (M $\geq$ 3)	Average Magnitude (M $\geq$ 3)	Probability (%)	Prediction (M)
22 August 1999	10	4.3	4.1	73.0	3.6
22 August 1999	9	3.4			
22 August 1999	9	4.0			
22 August 1999	5	3.7			
22 August 1999	1	4.0			
22 August 1999	5	5.0			

Table 11. Actual and estimated magnitude data for 23 August 1999.

Date	Depth (km)	Magnitude (M $\geq$ 3)	Average Magnitude (M $\geq$ 3)	Probability (%)	Prediction (M)
23 August 1999	1	3.1	3.3	69.4	3.4
23 August 1999	6	3.2			
23 August 1999	4	3.3			
23 August 1999	11	3.0			
23 August 1999	23	3.5			
23 August 1999	5	3.8			
23 August 1999	7	3.0			
23 August 1999	4	3.2			

Table 12. Actual and estimated magnitude data for 24 August 1999.

Date	Depth (km)	Magnitude (M $\geq$ 3)	Average Magnitude (M $\geq$ 3)	Probability (%)	Prediction (M)
24 August 1999	5	3.7	3.3	69.6	2.9
24 August 1999	9	3.0			
24 August 1999	8	3.1			
24 August 1999	6	3.2			
24 August 1999	7	3.0			
24 August 1999	16	3.7			
24 August 1999	1	3.2			
24 August 1999	1	3.1			

Table 13. Actual and estimated magnitude data for 25 August 1999.

Date	Depth (km)	Magnitude (M $\geq$ 3)	Average Magnitude (M $\geq$ 3)	Probability (%)	Prediction (M)
25 August 1999	1	3.1	3.4	70.1	2.8
25 August 1999	1	3.5			
25 August 1999	14	3.5			
25 August 1999	12	3.8			
25 August 1999	7	3.3			
25 August 1999	14	3.2			
25 August 1999	13	3.7			
25 August 1999	5	3.1			
25 August 1999	5	3.3			

Table 14. Actual and estimated magnitude data for 26 August 1999.

Date	Depth (km)	Magnitude (M ≥ 3)	Average Magnitude (M ≥ 3)	Probability (%)	Prediction (M)
26 August 1999	9	3.1	3.5	68.9	3.0
26 August 1999	2	3.1			
26 August 1999	1	3.6			
26 August 1999	7	3.0			
26 August 1999	5	3.2			
26 August 1999	6	3.7			
26 August 1999	3	4.1			
26 August 1999	5	3.6			
26 August 1999	5	3.6			
26 August 1999	5	3.5			

Table 15. Actual and estimated magnitude data for 27 August 1999.

Date	Depth (km)	Magnitude (M ≥ 3)	Average Magnitude (M ≥ 3)	Probability (%)	Prediction (M)
27 August 1999	9	3.3	3.3	71.1	3.0
27 August 1999	15	3.0			
27 August 1999	16	3.1			
27 August 1999	7	3.5			
27 August 1999	10	3.8			
27 August 1999	10	3.2			
27 August 1999	5	3.1			
27 August 1999	10	3.1			

Table 16. Actual and estimated magnitude data for 28 August 1999.

Date	Depth (km)	Magnitude (M ≥ 3)	Average Magnitude (M ≥ 3)	Probability (%)	Prediction (M)
28 August 1999	7	3.1	3.4	68.3	3.2
28 August 1999	5	3.6			
28 August 1999	5	3.3			
28 August 1999	22	3.3			
28 August 1999	9	3.6			
28 August 1999	5	3.7			
28 August 1999	9	3.5			
28 August 1999	9	3.2			
28 August 1999	9	3.0			

Table 17. Actual and estimated magnitude data for 29 August 1999.

Date	Depth (km)	Magnitude (M ≥ 3)	Average Magnitude (M ≥ 3)	Probability (%)	Prediction (M)
29 August 1999	5	3.3	3.7	70.3	3.4
29 August 1999	5	3.2			
29 August 1999	7	4.8			
29 August 1999	16	4.0			
29 August 1999	5	3.5			
29 August 1999	12	3.3			
29 August 1999	4	3.6			
29 August 1999	7	3.6			

Table 18. Actual and estimated magnitude data for 30 August 1999.

Date	Depth (km)	Magnitude (M ≥ 3)	Average Magnitude (M ≥ 3)	Probability (%)	Prediction (M)
30 August 1999	9	3.3	3.3	69.8	2.9
30 August 1999	4	4.0			
30 August 1999	5	3.2			
30 August 1999	8	3.2			
30 August 1999	1	3.0			
30 August 1999	5	3.1			
30 August 1999	5	3.0			
30 August 1999	8	3.5			
30 August 1999	10	3.1			
30 August 1999	5	3.2			
30 August 1999	13	3.1			
30 August 1999	4	3.3			

Table 19. Actual and estimated magnitude data for 31 August 1999.

Date	Depth (km)	Magnitude (M ≥ 3)	Average Magnitude (M ≥ 3)	Probability (%)	Prediction (M)
31 August 1999	17	5.2	3.5	70.3	3.0
31 August 1999	10	4.6			
31 August 1999	4	3.0			
31 August 1999	20	3.2			
31 August 1999	1	3.0			
31 August 1999	5	3.1			
31 August 1999	7	3.1			
31 August 1999	19	4.1			
31 August 1999	10	3.3			
31 August 1999	7	3.1			
31 August 1999	14	3.2			

For earthquakes occurring between 17 August 1999 and 31 August 1999, the evaluation of mean absolute percentage error (MAPE) was conducted for real magnitude data and predicted magnitude data. MAPE represents the average of absolute percentage errors between the real values and the corresponding predictions [37]. Its calculation formula is as follows (6) [37].

$$\text{MAPE} = (1/n) \times \Sigma \left| (\text{Real Value} - \text{Prediction}) / \text{Real Value} \right| \times 100 \quad (6)$$

- n represents the total number of data points.
- Real Value denotes the actual value compared to the predicted value.
- Prediction represents the predicted value.
- Σ indicates the summation symbol.

The mean absolute percentage error is 13.5%. The obtained MAPE chart for 17 August–31 August 1999 is presented in Figure 8.

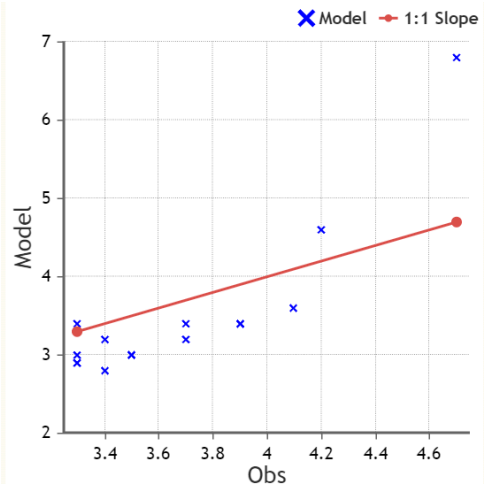

Figure 8. Mean absolute percentage error between 17 August and 31 August 1999.

6. Conclusions and Future Work

In this study, earthquake prediction and prediction rates were investigated using the RNN method for the Düzce Province, which is geographically located in the Marmara region of Turkey with GPS coordinates of 40°49′59″ N and 31°10′0″ E between the years 1990 and 2022. The dataset used included earthquake magnitude, depth, distance of the Moon from the Earth, b value, and d value. Although different methods are used in the studies, it can be seen that it is challenging to estimate 100% of the seismic data due to the irregular data structure.

This study found that the magnitude values estimated via the dataset created according to the research results and the applied method are close to the actual earthquakes' magnitudes.

It is expected that this study will be helpful for future earthquake prediction studies.

Author Contributions: Methodology, data curation, software, writing—original draft, validation, T.P.; Formal analysis, writing—review and editing, P.G., A.G. and A.A.H.; All authors have read and agreed to the published version of the manuscript.

Funding: This research received no external funding.

Institutional Review Board Statement: Not applicable.

Informed Consent Statement: Not applicable.

Data Availability Statement: The datasets generated and/or analyzed during the current study are available from the corresponding author on reasonable request.

Conflicts of Interest: The authors declare no conflict of interest.

References

1. Al-Baghdadi, J.A.; Mozahim Hamdoon, R.; Janan Yosief, F. Prediction the Locations of Future Earthquakes in Eastern Part of Iraq Using GIS Techniques. *MSE* **2020**, *745*, 012134. [CrossRef]
2. Deschamps, A.; Iannaccone, G.; Scarpa, R. The umbrian earthquake (Italy) of 19 september 1979. *Ann. Geophys* **1984**, *2*, 29–36.
3. Ishibashi, K. Status of historical seismology in Japan. *Ann. Geophys.* **2004**, *47*, 339–368. [CrossRef]
4. Van der Elst, N.J.; Shaw, B.E. Larger aftershocks happen farther away: Nonseparability of magnitude and spatial distributions of aftershocks. *Geophys. Res. Lett.* **2015**, *42*, 5771–5778. [CrossRef]
5. Purnomo, M.R.A. A Bayesian Reasoning for Earthquake Prediction Based on IoT System. *JPhCS* **2020**, *1471*, 012022. [CrossRef]
6. Azam, F.; Sharif, M.; Yasmin, M.; Mohsin, S. Artificial intelligence based techniques for earthquake prediction: A review. *Sci. Int.* **2014**, *26*, 1495–1502.
7. Núñez, J.L.M.; Lantada, A.S.D. Artificial Intelligence Aided Engineering Education: State of the Art, Potentials and Challenges. *Int. J. Eng. Educ.* **2020**, *36*, 1740–1751.
8. Brykov, M.N.; Petryshynets, I.; Pruncu, C.I.; Efremenko, V.G.; Pimenov, D.Y.; Giasin, K.; Sylenko, S.A.; Wojciechowski, S. Machine learning modelling and feature engineering in seismology experiment. *Sensors* **2020**, *20*, 4228. [CrossRef]

9. Faouzi, J.; Janati, H. pyts: A Python Package for Time Series Classification. *J. Mach. Learn. Res.* **2020**, *21*, 1–6.
10. Krischer, L.; Megies, T.; Barsch, R.; Beyreuther, M.; Lecocq, T.; Caudron, C.; Wassermann, J. ObsPy: A bridge for seismology into the scientific Python ecosystem. *Comput. Sci. Discov.* **2015**, *8*, 014003. [CrossRef]
11. Alves, E.I. Earthquake forecasting using neural networks: Results and future work. *Nonlinear Dyn.* **2006**, *44*, 341–349. [CrossRef]
12. Panakkat, A.; Adeli, H. Neural network models for earthquake magnitude prediction using multiple seismicity indicators. *Int. J. Neural Syst.* **2007**, *17*, 13–33. [CrossRef]
13. Adeli, H.; Panakkat, A. A probabilistic neural network for earthquake magnitude prediction. *Neural Netw.* **2009**, *22*, 1018–1024. [CrossRef] [PubMed]
14. Moustra, M.; Avraamides, M.; Christodoulou, C. Artificial neural networks for earthquake prediction using time series magnitude data or seismic electric signals. *Expert Syst. Appl.* **2011**, *38*, 15032–15039. [CrossRef]
15. Çam, H.; Duman, O. Yapay Sinir Ağı Yöntemiyle Deprem Tahmini: Türkiye Batı Anadolu Fay Hattı Uygulaması. *Gümüshane Univ. Electron. J. Inst. Soc. Sci. Gümüshane Univ. Sos. Bilim. Enst. Elektron. Derg.* **2016**, *7*, 227–248.
16. Özmen, B. Kastamonu ve yakın çevresi için deprem olasılığı tahminleri. *Turk. Jeol. Bul.* **2011**, *54*, 109–122.
17. Christopoulos, S.R.G.; Varotsos, P.K.; Perez-Oregon, J.; Papadopoulou, K.A.; Skordas, E.S.; Sarlis, N.V. Natural time analysis of global seismicity. *Appl. Sci.* **2022**, *12*, 7496. [CrossRef]
18. Sachs, M.; Turcotte, D.L.; Holliday, J.R.; Rundle, J. Forecasting earthquakes: The relm test. *Comput. Sci. Eng.* **2012**, *14*, 43–48. [CrossRef]
19. Dobrovolsky, I.P.; Zubkov, S.I.; Miachkin, V.I. Estimation of the size of earthquake preparation zones. *Pure Appl. Geophys.* **1979**, *117*, 1025–1044. [CrossRef]
20. Xiong, P.; Marchetti, D.; De Santis, A.; Zhang, X.; Shen, X. SafeNet: SwArm for earthquake perturbations identification using deep learning networks. *Remote Sens.* **2021**, *13*, 5033. [CrossRef]
21. Florios, K.; Contopoulos, I.; Tatsis, G.; Christofilakis, V.; Chronopoulos, S.; Repapis, C.; Tritakis, V. Possible earthquake forecasting in a narrow space-time-magnitude window. *Earth Sci. Inform.* **2021**, *14*, 349–364. [CrossRef]
22. Wu, Y.M.; Zhao, L. Magnitude estimation using the first three seconds P-wave amplitude in earthquake early warning. *Geophys. Res. Lett.* **2006**, *33*, L16312. [CrossRef]
23. Yamasaki, E. What we can learn from Japan's early earthquake warning system. *Momentum* **2012**, *1*, 2.
24. Nuttli, O. The effect of the Earth's surface on the S wave particle motion. *Bull. Seismol. Soc. Am.* **1961**, *51*, 237–246. [CrossRef]
25. Yılmaz, O.; Misli, Ç. Aristarchus Yöntemi ile Ay ve Güneş. *Fiz. Dunya. Derg.* **2016**, *1*, 1–8.
26. Gimsa, A. Development of the Distance Earth-Moon. *Int. J. Sci. Res. Manag.* **2020**, *8*, 10–13. [CrossRef]
27. Moon Distance Calculator. Available online: https://www.timeanddate.com/astronomy/moon/distance.html (accessed on 7 January 2022).
28. Ceylan, S. Marmara Depremlerinin Kaotik Özellikleri ve Fraktal Analizi. Ph.D. Thesis, İstanbul Teknik Üniversitesi, Fen Bilimleri Enstitüsü, Istanbul, Turkey, 2008.
29. Öztürk, S. Depremselliğin fraktal boyutu ve beklenen güçlü depremlerin orta vadede bölgesel olarak tahmini üzerine bir modelleme: Doğu Anadolu Bölgesi, Türkiye. *Gümüşhane Univ. Fen Bilim. Derg.* **2015**, *5*, 1–23. [CrossRef]
30. Öztürk, S. Elazığ Depremleri İçin Gutenberg-Rıchter B-Değeri Ve Fraktal Boyut Dc-Değerinin İstatistiksel Bir Analizi. In Proceedings of the 4th UluslararasıDeprem Mühendisliği ve Sismoloji Konferansı, Eskişehir, Turkey, 11–13 October 2017.
31. Polat, O.; Goek, E.; Yilmaz, D. Earthquake hazard of the Aegean extension region (West Turkey). *Turk. J. Earth Sci.* **2008**, *17*, 593–614.
32. Sherstinsky, A. Fundamentals of recurrent neural network (RNN) and long short-term memory (LSTM) network. *Physica D Nonlinear Phenom.* **2020**, *404*, 132306. [CrossRef]
33. Gao, Y.; Glowacka, D. Deep gate recurrent neural network. In Proceedings of the Asian Conference on Machine Learning, Hamilton, New Zealand, 16–18 November 2016; pp. 350–365.
34. Zhu, X.; Chu, J.; Wang, K.; Wu, S.; Yan, W.; Chiam, K. Prediction of rockhead using a hybrid N-XGBoost machine learning framework. *J. Rock Mech. Geotech. Eng.* **2021**, *13*, 1231–1245. [CrossRef]
35. Chen, Q.; Yang, H.; Guo, M.; Kannan, R.S.; Mars, J.; Tang, L. Prophet: Precise qos prediction on non-preemptive accelerators to improve utilization in warehouse-scale computers. In Proceedings of the Twenty-Second International Conference on Architectural Support for Programming Languages and Operating Systems, Xi'an, China, 8–12 April 2017; pp. 17–32.
36. Ariyo, A.A.; Adewumi, A.O.; Ayo, C.K. Stock price prediction using the ARIMA model. In Proceedings of the 2014 UKSim-AMSS 16th International Conference on Computer Modelling and Simulation, Cambridge, UK, 26–28 March 2014; pp. 106–112.
37. De Myttenaere, A.; Golden, B.; Le Grand, B.; Rossi, F. Mean absolute percentage error for regression models. *Neurocomputing* **2016**, *192*, 38–48. [CrossRef]